Mahmoud Jazayerifar, Meysam Namdari, Ryan Hamerly, Dodd Gray, Christopher Rogers, Kambiz Jamshidi

Feasibility study of optical parametric amplification using CMOS compatible ring resonators

Erstveröffentlichung in / First published in:

SPIE OPTO. San Francisco, 2017. Bellingham: SPIE, Vol. 10106 *[Zugriff am: 02.05.2019].*

DOI: https://doi.org/10.1117/12.2252635

PROCEEDINGS OF SPIE

SPIEDigitalLibrary.org/conference-proceedings-of-spie

Feasibility study of optical parametric amplification using CMOS compatible ring resonators

Mahmoud Jazayerifar, Meysam Namdari, Ryan Hamerly, Dodd Gray, Christopher Rogers, et al.

Mahmoud Jazayerifar, Meysam Namdari, Ryan Hamerly, Dodd Gray, Christopher Rogers, Kambiz Jamshidi, "Feasibility study of optical parametric amplification using CMOS compatible ring resonators," Proc. SPIE 10106, Integrated Optics: Devices, Materials, and Technologies XXI, 101060A (16 February 2017); doi: 10.1117/12.2252635

Event: SPIE OPTO, 2017, San Francisco, California, United States

Feasibility Study of Optical Parametric Amplification Using CMOS Compatible Ring Resonators

Mahmoud Jazayerifar[a], Meysam Namdari[a], Ryan Hamerly[b,c], Dodd Gray[b], Christopher Rogers[b], Kambiz Jamshidi[a]

[a]Integrated Photonic Devices Group, Technische Universität Dresden, Helmholtzstraße 16, 01069, Dresden, Germany;

[b]Edward L. Ginzton Laboratory, Stanford University, Stanford, CA 94305, USA

[c]National Institute of Informatics, Hitotsubashi 2-1-2, Chiyoda-ku, Tokyo 101-8402, Japan

ABSTRACT

In this paper, we analytically describe the parametric amplification in ring resonators using silicon and silicon nitride waveguides. Achievable gain and bandwidth of the ring-based amplifiers are studied taking into account the Kerr nonlinearity for silicon nitride and Kerr nonlinearity as well as two photon absorption and free carrier absorption for silicon waveguides. Both telecom and 2-µm wavelengths are investigated in case of silicon. An approach for obtaining the optimum amplifier design without initiating the comb generation has been introduced. It is shown that there is a trade-off between the input pump and amplifier bandwidth. It is estimated that using optimum designs an amplifier with a gain and bandwidth of 10 dB and 10 GHz could be feasible with silicon ring resonators in 2 µm.

Keywords: Optical parametric amplification, Kerr nonlinearity, Ring resonators

1. INTRODUCTION

Optical amplification is an important step toward enabling large scale CMOS compatible optical integrated circuits. The four wave mixing (FWM) process has been widely used in long (~100 m) fibers for amplification and phase conjugation [1-3]. Silicon and silicon nitride (SiN) waveguides have a much larger nonlinear coefficient compared to optical fibers which leads to much shorter lengths (~1 cm) [4-6]. However, due to the larger loss in these waveguides, the pump is severely depleted as it propagates in the waveguide, which limits the achievable parametric gain [5]. Using ring resonators, it is possible to collect a certain amount of pump power in the ring which is almost constant during propagation in the ring (because of the small size of the rings). This makes it possible to have a perfectly phase matched FWM process in the ring resonator at a certain wavelength (for anomalous dispersion). In other words, ring resonators can be used to compensate for the pump depletion-induced phase mismatch. Additionally, the collected effective pump power in the ring could be much larger than the input pump power which makes it possible to achieve a larger gain with a lower input pump power. These properties of ring resonators make them great candidates for amplification. However, as expected the resonant effect of ring resonators can severely limit the achievable bandwidth. Using ring resonators for amplification has been considered before [7]. However, in this paper we focus on the special case of parametric amplification in silicon and silicon nitride waveguides and analytically evaluate the performance of such amplifiers in terms of the expected gain and bandwidth. In our evaluations, we also consider the effect of nonlinear loss mechanisms in silicon: two photon absorption (TPA) and free carries absorption (FCA).

Fig. 1 shows the scenario which is considered in this paper. As can be seen in Fig. 1b both signal and pump should be located at resonance frequencies of the ring resonator.

Integrated Optics: Devices, Materials, and Technologies XXI, edited by Sonia M. García-Blanco,
Gualtiero Nunzi Conti, Proc. of SPIE Vol. 10106, 101060A · © 2017 SPIE
CCC code: 0277-786X/17/$18 · doi: 10.1117/12.2252635

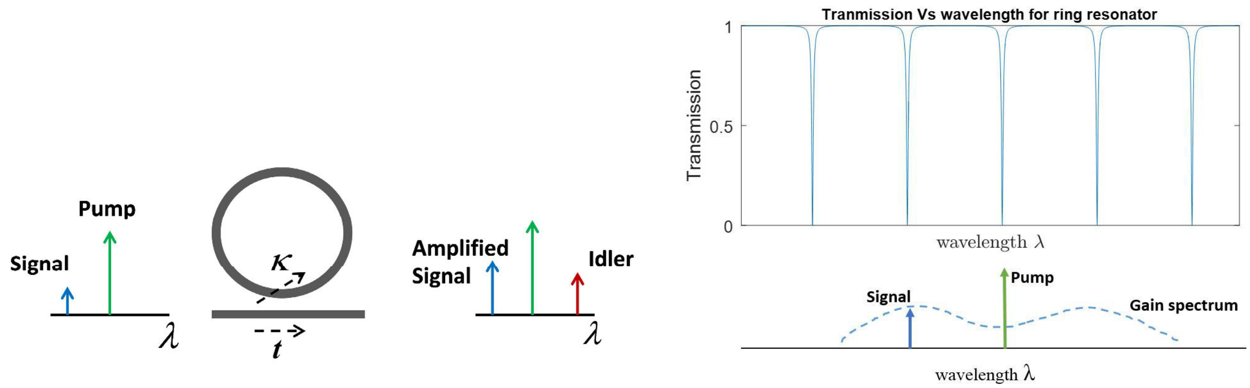

(a) (b)

Fig. 1. Optical parametric amplification with a ring resonator

2. SILICON NITRIDE RING RESONATOR AS AMPLIFIER

In SiN waveguides, there is no nonlinear loss mechanism at C-band wavelengths. If the input signal to the ring resonator and the output signal are denoted by A_{in} and A_o respectively, we have [8,9]:

$$\frac{A_o}{A_{in}} = \frac{ag-t}{1-tag} \tag{1}$$

where a, g, t are the loss per roundtrip, gain per roundtrip and inline coupling coefficient of the coupler, respectively. Note that in passive ring resonators g=1, whereas in active ring resonators g could be larger than 1. In order to have amplification we should have:

$$\left|\frac{A_o}{A_{in}}\right| > 1 \tag{2}$$

which leads to:

$$ag > 1 \tag{3}$$

The optical fields after parametric gain in perfect phase matching can be written as follows [1]:

$$\begin{bmatrix} A_{s,out} \\ A_{i,out}^* \end{bmatrix} = \begin{bmatrix} \cosh(\gamma P_{eff} L) & i\sinh(\gamma P_{eff} L) \\ -i\sinh(\gamma P_{eff} L) & \cosh(\gamma P_{eff} L) \end{bmatrix} \begin{bmatrix} A_{s,eff} \\ A_{i,eff}^* \end{bmatrix} \tag{4}$$

Where $A_{s,out}$, $A_{s,eff}$, $A_{i,out}$, $A_{i,eff}$ are the output signal, input signal, output idler, input idler, respectively as shown in Fig. 2.

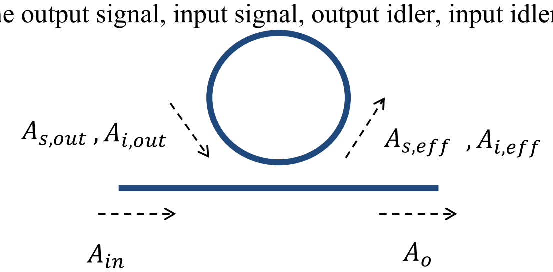

Fig. 2. Definition of $A_{s,out}$, $A_{s,eff}$, $A_{i,out}$, $A_{i,eff}$, A_{in}, A_o

γ, $P_{P,eff}$, L are the nonlinear coefficient, effective pump power in the ring and the ring circumference respectively. Combining equation (4) with the ring boundary conditions, for the scenario shown in Fig. 1, we have the following two equations:

$$\begin{cases} \left(-i\sinh(\gamma P_{eff}L)A_{s,eff} + \cosh(\gamma P_{eff}L)A^*_{i,eff}\right)at = A^*_{i,eff} \\ \left(\cosh(\gamma P_{eff}L)A_{s,eff} + i\sinh(\gamma P_{eff}L)A^*_{i,eff}\right)at + \kappa i A_{in} = A_{s,eff} \end{cases} \tag{5}$$

where k is the coupling coefficient of the coupler as shown in Fig. 1. $A_{s,eff}$ and $A_{i,eff}$ are the effective signal and idler fields circulating in the ring at the beginning of a roundtrip and * denotes the conjugation. Equation (5) leads to:

$$A_{s,eff} = \frac{1-at\cosh(\gamma P_{eff}L)}{1-2at\cosh(\gamma P_{eff}L)+(at)^2}\kappa i A_{in} \ , \ A_{i,eff} = \frac{\sinh(\gamma P_{eff}L)at}{1-2at\cosh(\gamma P_{eff}L)+(at)^2}\kappa A^*_{in} \tag{6}$$

For a passive ring ($P_{eff}=0$) the effective signal is as follows:

$$A_{s,eff} = \frac{1}{1-at}\kappa i A_{in} \tag{7}$$

By putting (6) in (4), we can calculate the ration $A_{s,out}/A_{s,eff}$, which gives us the gain per round trip and it is as follows:

$$g = \frac{\cosh(\gamma P_{eff}L) - at}{1 - at\cosh(\gamma P_{eff}L)} \tag{8}$$

Using (7) we can also obtain the effective pump power from the input pump power as follows:

$$P_{P,eff} = \frac{k^2 P_p}{(1-ta)^2} \tag{9}$$

where P_P is the input pump power. $P_{P,eff}$ will have its maximum at the critical coupling where $a=t$ [8]. In Fig. 3 this effective pump power is shown versus the input pump power for a ring resonator with a radius of 50 µm, loss of 1 dB/cm and different coupling coefficients. Due to the resonator's high finesse the effective power can be much larger than the input power.

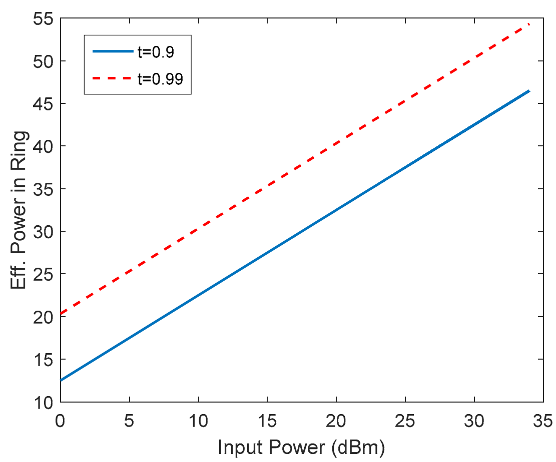

Fig. 3. Effective pump power in the ring versus the input pump power for SiN rings, (linear loss of 1 dB/cm, radius 50 µm)

In Fig. 4 the frequency response of the ring for different values of g is shown. This figure is just to show the concept and we will mention the achievable values of g in the rest of the paper in more detail. It can be observed that as g increases the resonance frequencies in which we have the minimum output power for passive rings, will change into the frequencies in which the gain is achieved.

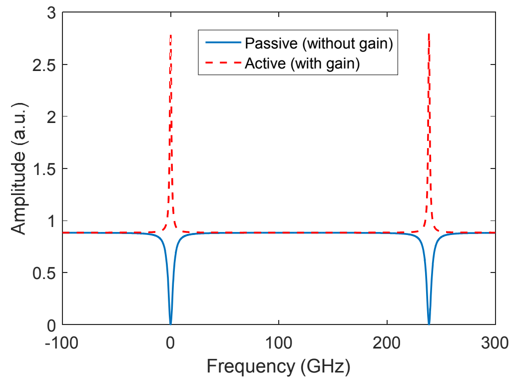

Fig. 4. Frequency response of passive and active ring resonators

In Fig. 5a we have plotted the input-output gain ($|A_o/A_{in}|^2$) versus the input pump power. We have assumed a ring with the radius of 50 μm, t=0.99, linear loss of 1 dB/cm, and nonlinear coefficient of 1.6 /W/m [5].

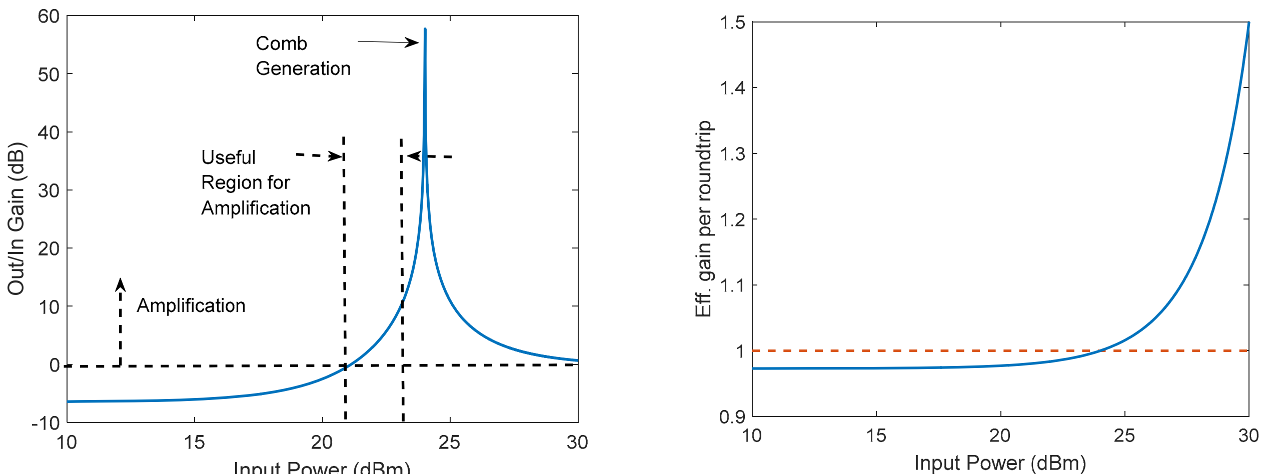

(a) (b)

Fig. 5. (a). Output/input gain versus the input pump power (ring radius = 50 μm, t=0.99, loss = 1 dB/cm and nonlinear coefficient = 1.6 /W/m). (b). *agt* (effective gain per round trip) versus the input pump power for the same ring as (a).

As expected, by increasing the input pump power the gain increases and at certain position the gain reaches its maximum value. This maximum corresponds to the case where *agt =1* in which comb generation occurs. The quantity *agt* can be called as the effective gain per round trip which is shown versus the input pump power in Fig. 5b It is observed that the maximum gain in Fig. 5a corresponds to the *agt* =1 in Fig. 5b

When *agt* =1, a random noise can circulate infinitely in the ring, and the ring could perform as a source. Obviously in this case the amplifier would suffer from a large distortion due to the interference with the generated comb frequency components. In order to avoid this condition, we should have:

$$agt < 1 \tag{10}$$

Therefore, to have an amplifier the two conditions (3) and (10) should be satisfied together which corresponds to the pump power levels larger than the value for which the gain is 0 dB and smaller than the comb generation threshold. This region is dented in Fig. 5a as the useful amplification region. We will describe this region in more details in section 4.

3. SILICON RING RESONATOR AS AMPLIFIER

Silicon waveguides suffer from TPA at both 1.55 μm and 2.0 μm. This is taken into account in our gain calculations in the following section. However, we neglect the three photon absorption (3PA) effect in these wavelengths. In the steady state condition, the density of the free carriers generated by the two-photon absorption (TPA) is given by [10]:

$$N_c = \frac{\tau_c \beta_{TPA}}{2h\nu}\left(\frac{P_{P,eff}}{A_{eff}}\right)^2 \tag{11}$$

Where β_{TPA}, A_{eff}, h, υ and τ_c are the TPA coefficient, effective area, Planck's constant, optical frequency and carrier lifetime. Having the carrier density, the free carrier absorption (FCA) is obtained from [11] according to the following empirical formula:

$$\alpha_{FCA} = aN_c^b + cN_c^d \tag{12}$$

Where *a, b, c, d* in different wavelengths are mentioned in [11]. The pump filed loss per round trip can be approximated as:

$$a_{Pump} = \exp\left(-\frac{\alpha L}{2} - \frac{\beta_{TPA}}{2A_{eff}} P_{eff} L - \frac{\alpha_{FCA} L}{2}\right) \tag{13}$$

This equation should be solved together with equation (9) to obtain the $P_{P,eff}$. This can be done numerically. In Fig. 6 the effective power is plotted versus the input power for a ring with the radius of 50 μm, loss of 1 dB/cm at two wavelengths of 1.55 μm and 2 μm for which we have β_{TPA} =0.85 cm/GW and β_{TPA} =0.2 cm/GW respectively [12]. We have also considered an effective area of A_{eff}=0.09 μm^2 and carrier life time of τ_C=20 ps which is achievable with a reversed-biased PIN junction [13]. It is also assumed that $t = 0.999$ which is close to the critical coupling for the linear loss case.

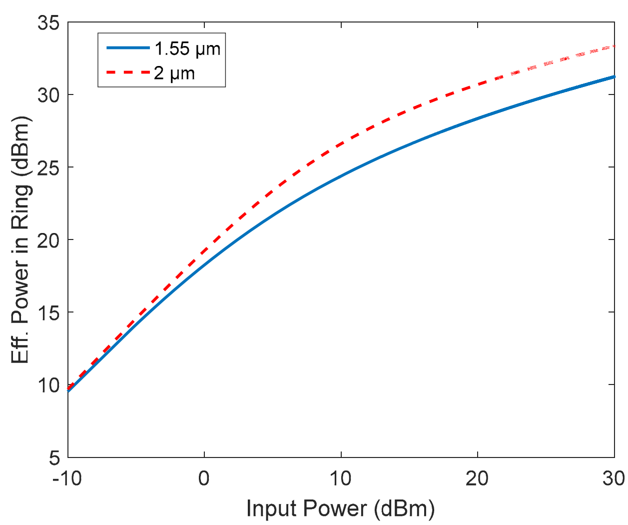

Fig. 6. Effective pump power in the ring versus the input pump power for silicon ring with a reversed bias PIN junction (carrier life time =20 ps), linear loss of 1 dB/cm, t=0.999, radius 50 μm in 1.55 μm (β_{TPA} =0.85 cm/GW) and 2 μm (β_{TPA} =0.2 cm/GW)

As expected, it is observed that the effective power starts to saturate as the input power increases due to the TPA and FCA. After obtaining the effective pump power, the corresponding loss can be obtained from the following equation:

$$a = \exp\left(-\frac{\alpha L}{2} - \frac{\beta_{TPA}}{A_{eff}} P_{eff} L - \frac{\alpha_{FCA} L}{2}\right) \tag{14}$$

where the FCA loss is calculated from (11) and (12). The corresponding gain (*g*) is obtained from (8) and finally the effective gain per roundtrip (*agt*) is obtained. In Fig. 7 the effective gain per roundtrip (*agt*) versus the input power is plotted. For this figure, we have assumed that the nonlinear index of refraction in 1.55 µm and 2 µm are 4.5×10^{-14} cm^2/W and 11×10^{-14} cm^2/W [12] leading to the nonlinear coefficient of γ=225 /W/m and γ=495 /W/m, respectively. It is observed that in 1.55 µm the effective gain per round trip can exceed unity indicating that the amplification could be feasible, however the effective gain per round trip does not reach very large values due to the degrading effect of TPA. However in 2 µm not only the TPA is smaller but also Kerr nonlinear coefficient is larger. Therefore, in 2 µm the gain reaches high values.

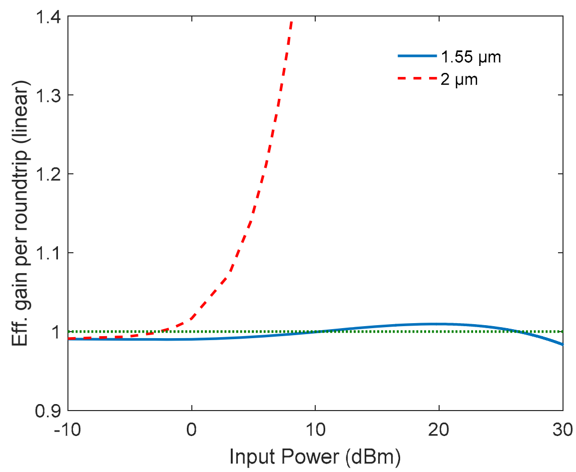

Fig. 7. The *agt* (effective gain per round trip) versus the input pump power for a ring with nonlinear index of refraction in 1.55 µm and 2 µm are 4.5×10^{-14} cm^2/W and 11×10^{-14} cm^2/W [6]

4. OPTIMIZATION OF GAIN AND BANDWIDTH

In the previous sections it was observed that using silicon nitride rings a large gain is achievable and using silicon ring resonators the amplification in both 1.55 µm and 2 µm could be possible provided that the carriers life time is reduced by a reversed bias PIN junction. In this section, we numerically discuss the amplifier gain and bandwidths which could be feasible with the silicon and silicon nitride ring resonators. In Fig. 8a we have considered a silicon nitride ring resonator and plotted the values *ag* and *agt* versus the input power. All numerical values are the same as section 2. As discussed in the previous sections, in order to avoid the comb generation we should have *agt*<1 which also limits *ag* as shown in Fig. 8a. It is observed that the maximum *ag* before running into the region where *agt*>1, is around 1.01. Therefore, in order to estimate the gain and bandwidth of the amplifier, we should consider a maximum *ag* of 1.01 as will be discussed in Fig. 9.We have plotted the same figure as Fig. 8a for silicon in 1.55 µm which is shown in Fig. 8b. The numerical values are the same as section 3 except that *t*=0.99. It is observed that due to the TPA the maximum gain is limited here and the maximum achievable *ag* is 1.005. As mentioned we have assumed *t*=0.99. In order to reach higher maximum gains, we can increase *t*. In Fig. 8c we have considered *t*=0.995. It is observed that a larger gain is achieved (~ up to 1.008) but the useful amplification region is limited here. Obviously in order to satisfy *ag*>1 and *agt*<1 together and to have a large region where these two conditions are satisfied together, it is better to have a small *t*. However, reducing *t* would decrease the gain per round trip. This reduction of the gain could be compensable by injecting a larger pump power in case there is no TPA (silicon nitride) or TPA is weak (silicon in 2 µm). However, in case of silicon in 1.55 µm injecting more pump power is not a solution. This leads to a trade-off between the useful range of pump powers for amplification and the maximum achievable gain. In Fig. 8d we have plotted the gain per round trip for a silicon ring resonator in 2 µm and *t*=0.99. It is interesting to observe that the required pump power is quite low due to the high nonlinear coefficient of silicon in 2 µm.

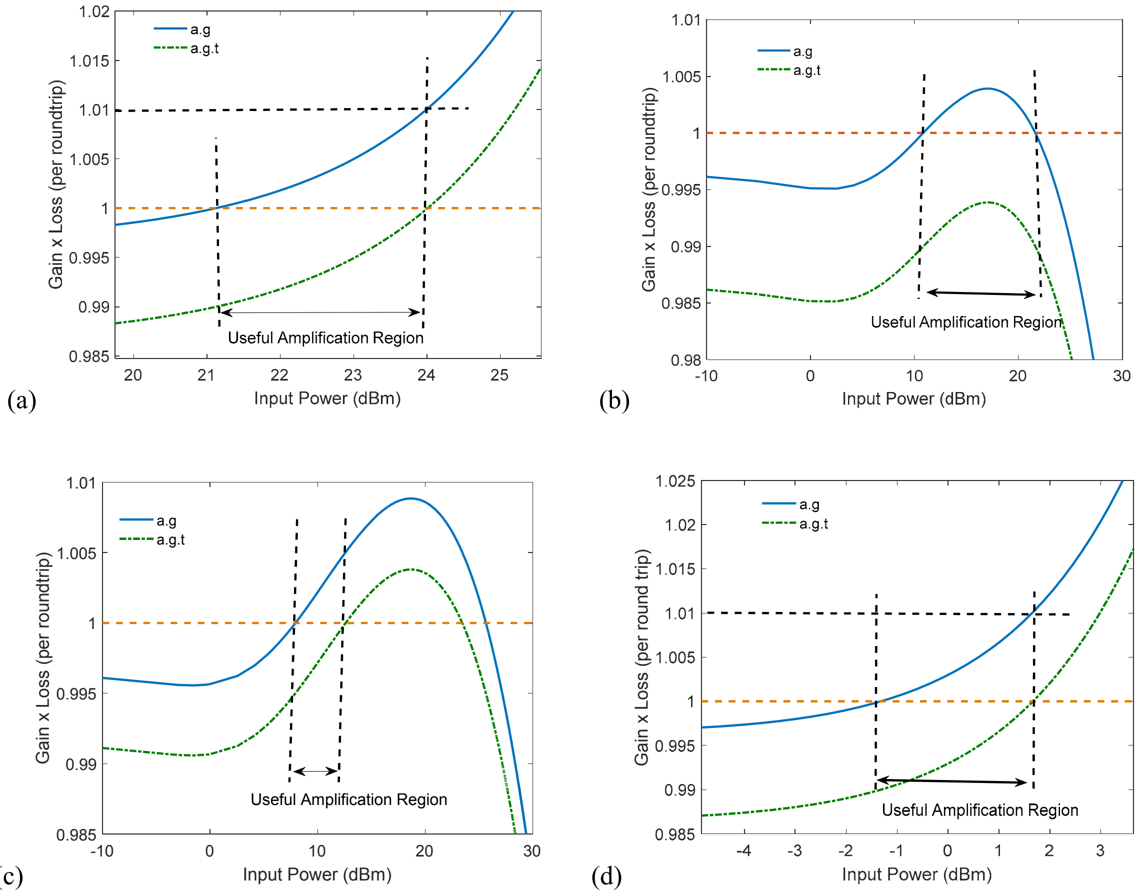

Fig. 8. Values of ag and agt in the vicinity of 1 versus the input pump power in (a) SiN ring with t=0.99 (b) Si with t=0.99 in 1.55 µm (c) Si with t=0.995 in 1.55 µm (d) Si with t=0.99 in 2 µm

The input-output transfer function (output power/input power) is as follows [8]:

$$T = \frac{t^2 - 2agt\cos(\varphi) + a^2g^2}{1 - 2agt\cos(\varphi) + a^2g^2t^2} \tag{15}$$

where $\varphi=\omega T_R$, and T_R is the cavity transit time and ω is the angular frequency. Using equation (15) we can calculate the 3-dB Full-width half-maximum (FWHM) bandwidth.

In Fig. 9 we have plotted the output/input gain and bandwidth versus ag. As can be observed, there is trade-off between gain and bandwidth and as gain increases the bandwidth decreases and in the case the gain tends to infinity the bandwidth tends to zero.

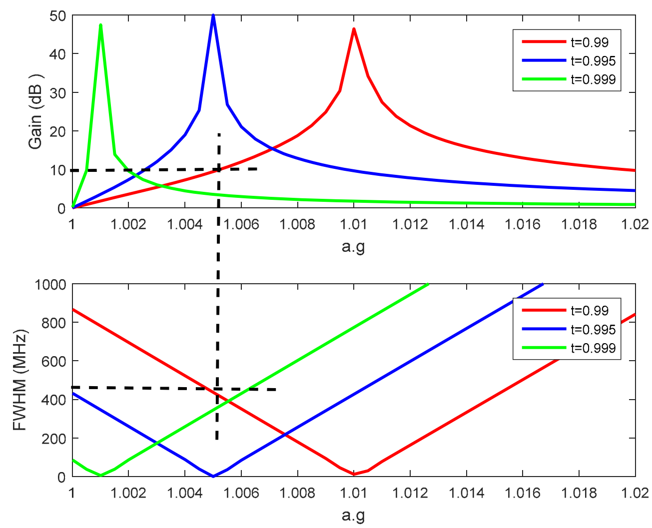

Fig. 9. Gain and FWHM bandwidth versus *ag* for different coupling values (ring radius = 50 µm)

According to Fig. 8 in most of the cases we were able to have *ag* value up to 1.01 without running into comb generation region. In Fig. 9 for this range of *ag* we have plotted the input-output gain and bandwidth. It is observed that for *t*=0.99 and a gain of 10 dB the bandwidth is around 440 MHz which is not a large bandwidth. From Fig. 9, it is realized that by increasing *ag* it possible to achieve a larger bandwidth. However, as discussed before increasing *ag* without running into comb generation, would require a larger *t* and consequently a larger input pump power. Considering the fact that the required pump power in silicon in 2 µm were low in Fig. 8, we realize that in order to increase the bandwidth it is better to employ silicon rings in 2 µm and to decrease *t*. We have followed this approach in Fig. 10 for *t*=0.8. It is observed that with *t*=0.8 and a pump power of 26 dBm we are still in the amplifier region. With *ag*=1.24 and *t*=0.8 we achieve a bandwidth of 10 GHz according to Fig. 10b.

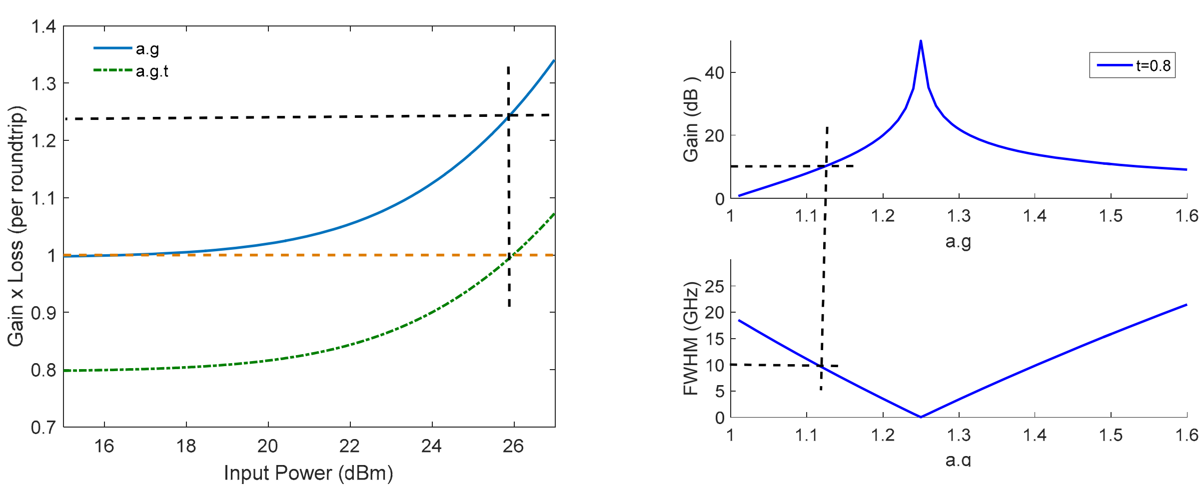

(a) (b)

Fig. 10. (a) Values of *ag* and *agt* in the vicinity of 1 versus the input pump power for a silicon ring in 2 µm (*t*=08, radius=50 µm) (b) Gain and FWHM bandwidth versus *ag* for a silicon ring in 2 µm (t=0.8, ring radius of 50 µm)

5. CONCLUSION

The parametric amplification mechanism in ring resonators is analytically explained. In the case of silicon, the effect of nonlinear loss mechanisms on the gain is analytically studied. An approach for gain and bandwidth optimization in ring resonators was introduced. A useful amplification region, where the comb generation does not occur, has been identified. It was that using reversed bias PIN junctions, it would be possible to achieve amplification in both 1.55 µm and 2 µm. However, the achievable gain in 1.55 µm is rather limited due to the dominance of TPA. We finally showed that silicon ring resonators in 2 µm can be designed such that a gain of 10 dB and a bandwidth of 10 GHz are achievable.

ACKNOWLEDGEMENTS

This work is supported, in part, by the German Research Foundation (DFG) in the context of the collaborative research center (CRC) 912 “Highly adaptive energy-efficient computing” (HAEC).

REFERENCES

[1] Andrekson, Peter A. "Phase-sensitive fiber-optic parametric amplifiers and their applications." *Asia Communications and Photonics Conference*. Optical Society of America, 2012.

[2] Andrekson, P.A., Petropoulos, P., Radic, S., Peucheret, C. and Jazayerifar, M.,"Fiber optical parametric amplifiers in optical communication systems." *Laser & photonics reviews* 9(1), 50-74 (2015).

[3] Da Ros, F., Sackey, I., Elschner, R., Richter, T., Meuer, C., Nölle, M., Jazayerifar, M., Petermann, K., Peucheret, C. and Schubert, C., "Kerr nonlinearity compensation in a 5× 28-GBd PDM 16-QAM WDM system using fiber-based optical phase conjugation." *40th European Conference on Optical Communication* (ECOC 2014). *IEEE*, (2014).

[4] Foster, M.A., Turner, A.C., Sharping, J.E., Schmidt, B.S., Lipson, M. and Gaeta, A.L., “Broad-band optical parametric gain on a silicon photonic chip.” *Nature* 441(7096), 960-963 (2006).

[5] Jazayerifar, M., Jamshidi, K., “phase sensitive parametric process in silicon Nano-waveguides at C-band wavelengths,” *IEEE Photonics Journal* 8 (5), 1-9 (2016).

[6] Jazayerifar, M., Jamshidi, K., “Optical Sampling with CMOS Compatible Waveguides in C-Band Wavelengths.” *In CLEO: Science and Innovations, Optical Society of America.* (2016)

[7] Dumeige, Y., Trebaol, S., Ghişa, L., Nguyen, T.K.N., Tavernier, H. and Féron, P., "Determination of coupling regime of high-Q resonators and optical gain of highly selective amplifiers." JOSA B 25(12), 2073-2080 (2008).

[8] Yariv, A., “Critical coupling and its control in optical waveguide-ring resonator systems,” in *IEEE Photonics Technology Letters* 14(4), 483-485 (2002).

[9] Bogaerts, W., De Heyn, P., Van Vaerenbergh, T., De Vos, K., Kumar Selvaraja, S., Claes, T., Dumon, P., Bienstman, P., Van Thourhout, D. and Baets, R., “Silicon microring resonators.” *Laser & Photonics Reviews* 6(1), 47-73 (2012).

[10] Rukhlenko, I.D., Premaratne, M. and Agrawal, G.P., "Nonlinear silicon photonics: analytical tools." IEEE journal of selected topics in quantum electronics 16(1), 200-215 (2010).

[11] Nedeljkovic, M., Soref, R. and Mashanovich, G.Z., “Free-Carrier electrorefration and electroabsorption modulation predictions for silicon over the 1-14-infrared wavelength range.” *IEEE Photonics Journal* 3(6), 1171-1180 (2011).

[12] Bristow, A.D., Rotenberg, N. and Van Driel, H.M., “Two-Photon absorption and Kerr coefficients of silicon for 850-2200nm.” *Applied Phys. Let*. 90(19), 191104 (2007).

[13] Gajda, A., Zimmermann, L., Jazayerifar, M., Winzer, G., Tian, H., Elschner, R., Richter, T., Schubert, C., Tillack, B., and Petermann. K., "Highly efficient CW parametric conversion at 1550 nm in SOI waveguides by reverse biased pin junction." *Optics express* 20(12), 13100-13107 (2012).